A&A 478, 907–913 (2008)
DOI: 10.1051/0004-6361:20078641

Astronomy & Astrophysics

Observations of H_α surges and ultraviolet jets above satellite sunspots

H. D. Chen[1,2], Y. C. Jiang[1], and S. L. Ma[1,2]

[1] Yunnan Observatory/National Astronomical Observatories, Chinese Academy of Sciences, Kunming 650011, PR China
e-mail: hdchen@ynao.ac.cn
[2] Graduate School of Chinese Academy of Sciences, Beijing 100049, PR China

Received 10 September 2007 / Accepted 30 November 2007

ABSTRACT

Aims. To know more about the physical origin of surges and jets, we investigated seven successive surge events, which occurred above the satellite sunspots of active region NOAA 10720 on 2005 January 15.
Methods. Using data from the *Transition Region and Coronal Explorer* (TRACE), *Big Bear Solar Observatory* (BBSO) and *Solar and Heliospheric Observatory* (SOHO), we present a detailed study of the surges and their relations with the associated small arch filament, UV jets, flares and photospheric longitudinal magnetic fields.
Results. The seven H_α surges we studied repeatedly occurred where the photospheric longitudinal fluxes of opposite magnetic polarities emerged, converged and were canceled by each other. Correspondingly, a small satellite spot emerged, decayed and disappeared during a period of about 2 hours in the white-light observations. In morphology, all surges displayed almost linear ejective structures. Their dynamic properties, such as the transverse velocity, projected maximum length and lifetime, varied in wide ranges. They are 30–200 km s^{-1}, 38 000–220 000 km and from several to tens of minutes, respectively. Correspondingly, the intensities of their correlated microflares were different too. The surges of major velocities or maximum lengths seemed to be accompanied by processes of more energy release. Prior to these surge events, a small H_α arch filament connecting the opposite flux elements was found at the base region. Instead of erupting completely, it gradually disappeared during the surges. Its role in the surge activities is very like a bipolar flux, which contained the cool plasma and reconnected with the ambient magnetic fields. In 1600 Å, three surge events exhibited the composite structures of bright jets and nearby small flaring loops, which provides direct evidence of magnetic reconnection origin of the surges. A careful comparison revealed that the ends of the arch filament, the UV jets and the small flaring loops just corresponded to the interacting longitudinal fluxes in the photosphere.
Conclusions. These observational results support the magnetic reconnection model of surges and jets.

Key words. Sun: activity – Sun: chromosphere – Sun: magnetic fields – Sun: UV radiation

1. Introduction

Surges are phenomena in which dark dense mass are ejected in the solar atmosphere from chromospheric into coronal heights. Usually, they appear as straight or slightly curved ejective structures, and they often recur (Bruzek & Durrant 1977; Li et al. 1996). At first, they were studied in H_α and were called "H_α absorption markings" by Newton (Newton 1934, 1942). They have a typical size of $(5–20)\times10^4$ km, a transverse velocity of 50–200 km s^{-1} and a lifetime of 10–20 min. The rotational or helical motions were, on occasions, also observed in surge activity (Gu et al. 1994; Canfield et al. 1996).

Similar ejection phenomena at other wavelengths, such as UV, EUV and X-ray jets, have also been studied by a number of authors (Schmahl 1981; Schmieder et al. 1984; Švestka et al. 1990; Shibata et al. 1992; Schmieder et al. 1993; Shimojo et al. 1996; Zhang et al. 2000; Asai et al. 2001). Regarding the question about the temporal and spatial relationships between surges and jets, some authors have given different, and even opposite results (see Rust et al. 1977; Schmieder et al. 1988; Shibata et al. 1992). However, this confusion may be caused by different spatial and temporal resolutions of the UV, EUV and X-ray data used in the comparisons, which has been discussed in detail by Liu & Kurokawa (2004). Recent observational results showed that surges and jets should be associated with each other and represent different temperature plasma ejections along different magnetic field lines (Chae et al. 1999; Liu & Kurokawa 2004; Chen et al. 2005; Jiang et al. 2007).

Surges are well correlated with certain types of photospheric magnetic features, such as satellite spots (Rust 1968), emerging magnetic flux (Roy 1973; Kurokawa & Kawai 1993) and moving magnetic bipoles (Canfield et al. 1996). In the statistical study by Shimojo et al. (1998), it was found that X-ray jets also favored the regions of evolving magnetic flux (increasing or decreasing). More recently, Chae et al. (1999), Zhang et al. (2000), Yoshimura et al. (2003) and Liu & Kurokawa (2004) studied the surges in emerging flux regions and found that the preexisting field was canceled by newly-emerging flux of opposite polarity at the bases of surges. Using multi-wavelength observations, Jiang et al. (2007) examined three successive surge events in the quiet-sun region and also found the similar results. In this paper, we emphasize the investigation of a series of H_α surges above the satellite sunspots of an active region. We expect to learn more about the relation between surges and the evolution of photospheric spots.

In theory, many models were devoted to the interpretation of surges and jets (see the detailed discussions by Schmieder et al. 1995 and Canfield et al. 1996). However, more and more observational results seem to support the magnetic reconnection

model (Kurokawa & Kawai 1993; Shibata et al. 1994; Canfield et al. 1996). In this model, first, reconnection occurred between the newly-emerging flux and the preexisting ambient field. Then, the hot plasma was heated by the reconnection and transferred along the open and closed field lines, which led to jet and small flaring loops respectively; while the cool plasma was ejected by the tensile strength of the reconnected field and formed surge simultaneously. This scenario has been reproduced by the numerical simulations of Yokoyama & Shibata (1995, 1996).

In the associated subflares or microflares, the flaring loop structures or loop brightenings were frequently observed to appear and were somewhat separate from the exact footpoints of surges and jets. As a result, some authors regarded it as evidence of the magnetic reconnection surge model (Shibata et al. 1994; Schmieder et al. 1995; Canfield et al. 1996). However, some aspects about the flaring loops, such as their spatial relation with the photospheric magnetic fields, have not been studied in detail as yet. As for the surge events on 2005 January 15, the high spatial resolution data from TRACE and BBSO provide us with the opportunity to study this aspect. In the next section, we describe the observations and data processing. This is followed by a detailed study of the surges and their associated activities, including the disappearance of an H_α arch filament, small flares, UV jets and the evolutions of photospheric longitudinal fields and sunspots etc. Finally, we give the conclusions and discussions and try to explain the observational results by the magnetic reconnection surge model.

2. Observations and data processing

Simultaneous observations by TRACE (Handy et al. 1999; Schrijver et al. 1999) and BBSO were made of the active region NOAA 10720 on 2005 January 15 from 17:00 to 23:00 UT. At the time of observations, the active region was approximately located at a disk position 50″ west and 297″ north from disk center. TRACE observed the region in ultraviolet (UV) passband (centered mainly at λ = 1600 Å) and a broadband white-light (WL) passband. The 1600 Å channel has a temperature sensitive range of $(4.0–10)\times10^3$ K and is more sensitive to a higher temperature of $\sim10^5$ K during flares (Saba et al. 2006). The image scale is 0.″5 per pixel. Together with considering the aperture of the telescope (MTF), it implies a spatial resolution of 1″. The image sequences were processed with the standard IDL procedures in Solar Software (SSW) (Freeland & Handy 1998). It corrects missing pixels, replaces saturated pixels with values above 4095, subtracts the dark field and corrects for the flat field. The image brightness was normalized by the exposure time.

The BBSO observations used in the current study were (1) full-disk H_α images observed by the Singer telescope with a spatial resolution of 2″ (Denker et al. 1999) and a cadence of 1 min; (2) line-of-sight magnetograms (Stokes V images) obtained by the Digital Vector Magnetograph system (DVMG) with a pixel size of 0.″6 and a cadence of several minutes, however some data gaps of tens of minutes also exist; and (3) region H_α data from the 25 cm vacuum reflector with the same pixel size as the magnetograms, but better than that of the full-disk H_α images. Due to the incorrect clock on the Singer telescope on that day, we also examined the H_α data from the Polarimeter for Inner Coronal Studies (PICS) at the Mauna Loa Solar Observatory (MLSO) to correct the observing time of the BBSO full-disk H_α data. The BBSO DVMG is a filter-based magnetograph which uses a $\frac{1}{4}$ Å Zeiss H_α filter retuned to the magnetically sensitive Ca I line at 6103 Å (Spirock et al. 2001). Both full-disk H_α images and magnetograms were corrected by dark and flat field. To ensure the data reliability, we omitted most magnetograms affected by bad weather or certain instrumental factors.

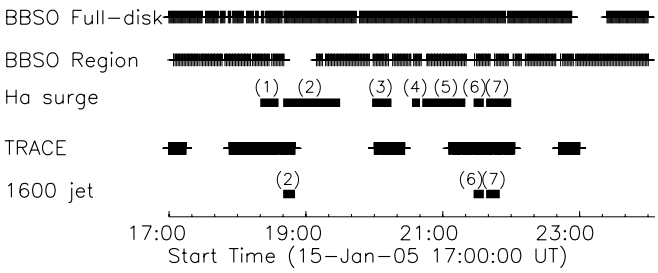

Fig. 1. The observation logs of the BBSO full-disk, region H_α and TRACE 1600 Å data are symbolically described in the first, second and fourth rows, respectively. In the special form, each observed time is represented by a plus sign. The third and the fifth rows show the ejections seen in the H_α images and in the UV images, respectively.

In addition, we used one line-of-sight magnetogram from *Michelson Doppler Imager* (MDI) instrument (Scherrer et al. 1995) on board SOHO. Its pixel size is 2″. It is necessary and important to co-align the data from different instruments. Using an MDI continuum image, we aligned the TRACE WL images with the BBSO and MDI magnetograms. To perform the co-alignments among the BBSO H_α, TRACE 1600 Å and magnetograms data, we used recognition of solar features, such as small sunspots or chromospheric plages and their corresponding photospheric magnetic fields. The accuracy in all co-alignments was better than 2″.

From 18:00 to 22:00 UT on January 15, we found seven H_α surges and three associated 1600 Å jets altogether. In Fig. 1, the times of H_α (including the full-disk and region) and UV observations are summarized, where each time is represented by plus sign. The numbered thick lines in the third and fifth rows show the times when the ejections are distinctly identified at H_α and 1600 Å, respectively. We mainly researched events 6 and 7 which occurred around 21:30 and 21:40 UT respectively, because both H_α and UV observations covered them well.

3. Results

In this study, all surge events occurred above the same satellite sunspots region which developed on the northeast edge of the large and complex active region – NOAA AR 10720. The BBSO full-disk H_α images (Fig. 2) show their almost linear morphological structures when they were ejected. The NOAA AR 10720 was located at the lower right corner in the images. Some observed properties of the seven H_α surges and the two 1600 Å jets are listed in Table 1. According to our calculations, their projected maximum lengths range from 38 000 to 220 000 km, their transverse velocities are 30–200 km s^{-1} and their lifetimes are from several to tens of minutes. Asai et al. (2001) took statistics of similar features of eight surges, which were ejected from a light bridge in a sunspot umbra. In contrast to their results, the dynamic characteristics of the surges we studied vary in wide ranges, while those of their surges are relatively even.

Using the full-disk H_α images and calculating the total H_α intensity in the area enclosed by the box in the 18:29 UT panel of Fig. 2, we found that each surge was accompanied by an H_α brightening at its foot, which can be called subflare or microflare. The H_α flux time profile is shown in panel a of Fig. 6, in which

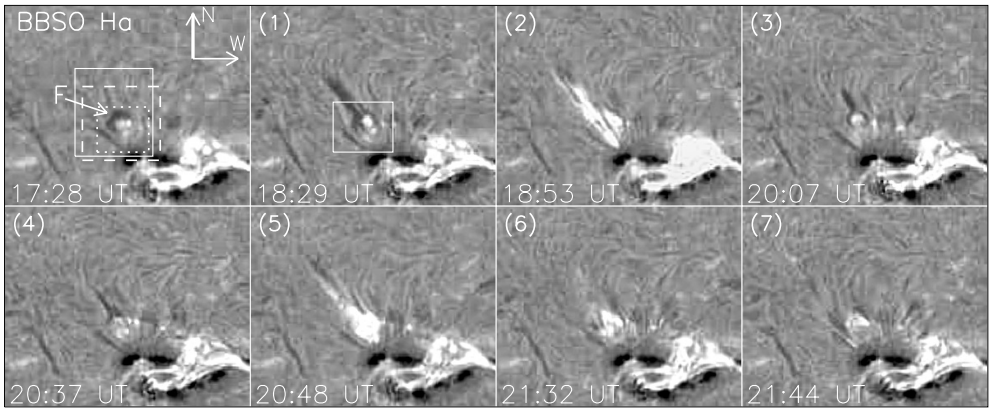

Fig. 2. BBSO full-disk H_α images show seven H_α surges occurred at the same location. For convenience of comparison, we give one H_α image prior to the surge activities in the top left panel. The symbol "F" indicates the small arch filament at the base of the subsequent surges. The field of view (FOV) is $300'' \times 245''$. The solid, dashed and dotted boxes in the first panel indicate the FOVs of Figs. 4 and 5, Figs. 7 and 3, respectively. The white box in the 18:29 UT panel outlines the area where we calculated the H_α flux, whose time profile is shown in Fig. 6. North is to the top and west to the right, which is the same for all the following figures.

Table 1. Transverse velocity and projected maximum length of H_α surges and UV jets.

Event	Time (UT)	Transverse velocity (km s^{-1})	Projected maximum length (Mm)
1...	18:29	83.1	69.8
2...	18:53	104.3	214.1
3...	20:07	66.0	47.2
4...	20:37	37.6	45.4
5...	20:48	195.3	189.4
6...	21:32	82.5	38.3
7...	21:44	80.9	102.8
		UV 1600 Å	
6...	21:30	127.9	65.2
7...	21:40	...	57.6

the dashed lines indicate the times when the surges began to come forth in H_α. By comparison between Table 1 and panel a of Fig. 6, we can see that the intensities of the associated microflares were different too. As a whole, the surges of major velocities or maximum lengths seemed to correspond to more energy release. Prior to these surges, a small arch filament, which is labelled "F" in the top left panel, was found at their base. As for three minor surges, i.e. the events 1, 3 and 4, it is apparent that cool plasma rose from the filament and supplied material for dark surges. However, in the two major surge activities 2 and 5, due to very intense energy release, a large number of bright features were ejected from the base region, which completely hid the evolution of F. Before surges 6 and 7 started, the filament F was effectively invisible in H_α (see Fig. 5).

By examining the movies of BBSO line-of-sight magnetograms and TRACE white-light images, we investigated the evolutions of the photospheric magnetic fields and sunspots at the base of the surges, which is shown in Fig. 3. The field of view (FOV) of Fig. 3 is indicated by the dotted box in the top left panel of Fig. 2. Firstly, it must be mentioned that although we have omitted most magnetograms affected by bad seeing, two fuzzy magnetograms observed at 18:27 and 21:40 UT were still selected and shown in Fig. 3. For only morphological study, we think that it would not affect the result very much. As a matter of convenience, three small flux regions are marked as "A", "B" and "C", which are enclosed by three white dotted circles in the

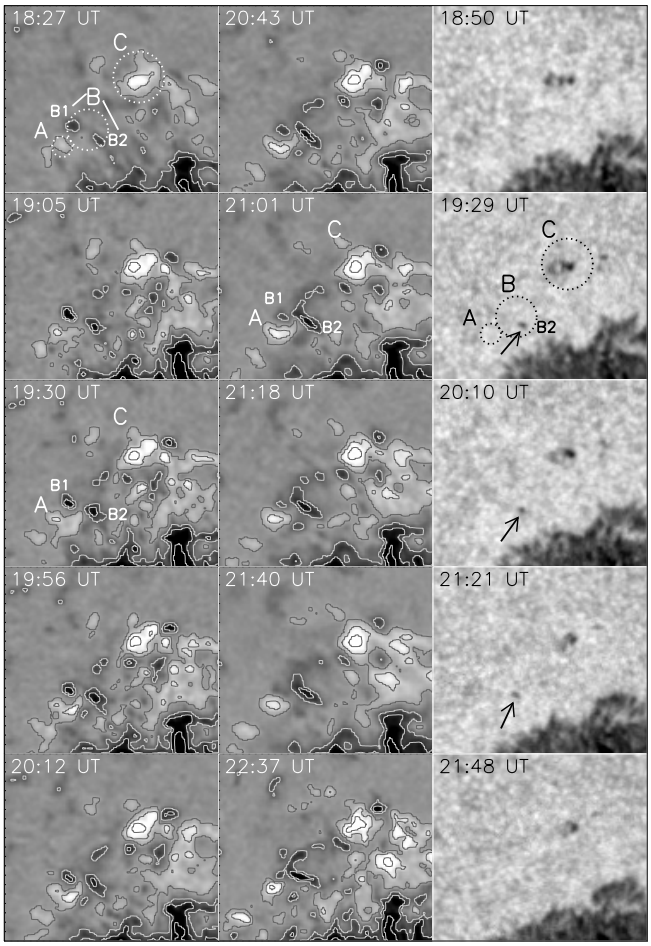

Fig. 3. BBSO line-of-sight magnetograms (*left and middle columns*) superposed with their contours and TRACE white-light images (*right column*) showing the evolutions of the photospheric longitudinal fields and sunspots. The levels of the contours are ±80, 200, 400 G. The black arrows point to the quickly emerging and disappearing spot corresponding to the negative flux B2. The FOV is $63'' \times 55''$.

18:27 UT panel. Among them, the region B was composed of two negative flux elements – "B1" and "B2". For better comparison, by plotting three black dotted circles in the 19:29 UT

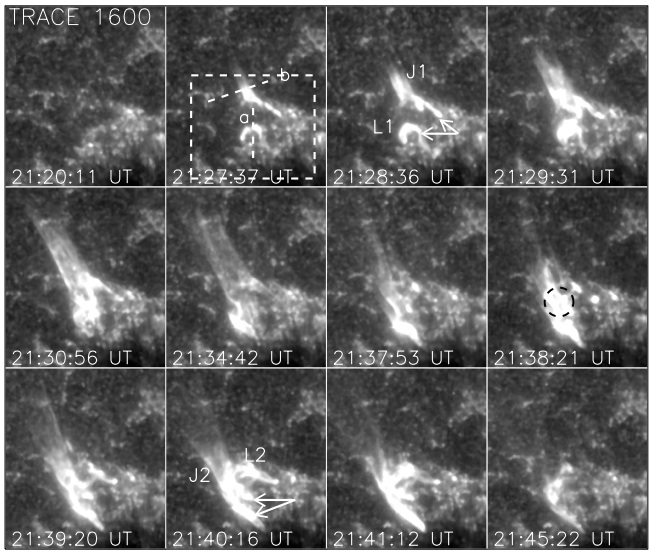

Fig. 4. Time sequence of TRACE 1600 Å images. The dashed box indicates the region calculated for the time profile of 1600 Å flux in Fig. 6. The dashed lines a and b point out where we computed the thickness of L1 and the width of J1, respectively. The FOV is 95″ × 107″.

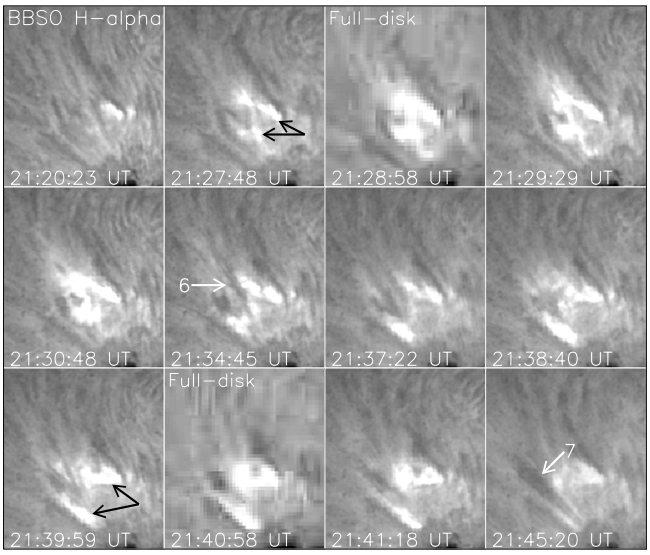

Fig. 5. Time sequence of BBSO region H_α images. Due to the data gap, two full-disk H_α images are shown in the 21:28:58 and 21:40:58 UT panels as complements. The FOV is the same as that of Fig. 4.

panel, we also highlighted where the areas corresponding to the flux regions A, B and C are in the WL images.

From 18:27 to 22:37 UT, the four magnetic flux elements A, B1, B2 and C evolved in different ways, respectively. Before 21 UT, the positive flux A seemed to emerge from under the photosphere continually, but then gradually decayed. In the region B, the flux B1 continued decaying, while B2 seemed to grow at first and not change very much after 21 UT. From 19:05 to 21:18 UT, it is obvious that the activities of collision and cancellation occurred between the positive flux A and the negative flux B1 and B2. Until 21:18 UT, B1 had become very weak in the magnetogram. As to the flux C, it is hard to identify its strength change only from the magnetograms, but in the WL images, the decay of its corresponding sunspots is clear from 18:50 to 21:48 UT. An interesting finding is that a small satellite sunspot emerged, decayed and disappeared in the area corresponding to the flux B2, between 19:29 and 21:48 UT. Due to the data gap between 18:50 and 19:29 UT in TRACE WL observations, we do not know at what exact time the spot started to emerge in photosphere. The three arrows in the WL images of Fig. 3 point to the spot evolving rapidly.

Due to good H_α and UV observations on surge events 6 and 7, we investigated the two events in detail. Time sequences of TRACE 1600 Å and BBSO H_α images are shown in Figs. 4 and 5, respectively. They have the same FOV, which is indicated by the solid box in the top left panel of Fig. 2. Interestingly, in the 1600 Å images, we found that two small bright loops L1 and L2 appeared near the footpoints of the two UV jets J1 (event 6) and J2 (event 7), respectively.

One gap (indicated by the arrows in the 21:28:36 UT panel) with a width of ∼11 000 km existed between the footpoints of J1 and L1. As to J2 and L2, the gap (indicated by the arrows in the 21:40:16 UT panel) between their footpoints is about 7000 km. Without taking account of the projection effect, these values should be only the lower limits of the actual distances. In the study of Shimojo et al. (1996), 27% of 100 X-ray jets showed a gap of more than 10^4 km between the exact footpoint of the jet and the brightest part of the associated flare. Our results are comparable with theirs. When the UV jet J1 was ejected along the open field lines with an apparent velocity of more than 100 km s^{-1}, its width continued to increase at a speed of ∼39 km s^{-1}. Meanwhile, the small loop L1 also increased its thickness with an apparent velocity of ∼27 km s^{-1}. The two dashed lines "a" and "b" (in the 21:27:37 UT panel) indicate where we calculated the thickness of L1 and the width of J1. Shibata et al. (1994) reported a gigantic X-ray jet with a maximum length of more than 3×10^5 km. A bright loop appeared nearby the footpoint of the X-ray jet and increased its height continuously. However, the loop ascending speed in their observations was only about 3 km s^{-1}, which is almost an order of magnitude smaller than that of L1 in this study. As for the second UV jet J2 we studied, it began to appear in 1600 Å around 21:38 UT, only 12 min after the appearance of J1. From the 21:38:21 UT panel, we can clearly see that a sudden UV brightening (indicated by a dashed circle) occurred between the subsequent J2 and L2, which was just the onset of event 7. Due to very low intensity of the moving front, it is hard to obtain the translational velocity of J2. Compared with J1 and L1, two main difference were found between the two jets. Firstly, the relative spatial relationship between J1 and L1 is different from that between J2 and L2. L1 was southeast of J1, while L2 was northwest of J2. This indicates that event 7 was not a simple recurrence of event 6, although they occurred at the same location. Secondly, as J2 and L2 developed, it is hard to distinguish their widening or thickening variations, while that can be clearly seen on J1 and L1. One possible reason is that J2 and L2 are located in a plane that is nearly parallel to the line of sight. It should be mentioned that although the UV observation did not cover event 2 well, we can still see the composite structure of bright jet and small flaring loop at the beginning of this event, which was very similar to event 6.

In H_α center-line images (Fig. 5), two associated dark surges are marked with "6" and "7" in the 21:34:45 and 21:45:20 UT panels, reflecting that they are the sixth and seventh events we studied. The two surges 6 and 7 began to appear around 21:33 and 21:43 UT respectively, which were a few minutes later than their correlated UV jets J1 and J2. Moreover, we observed the chromospheric counterparts of the footpoints of J1 and J2 and those of L1 and L2, which can be easily identified as four bright

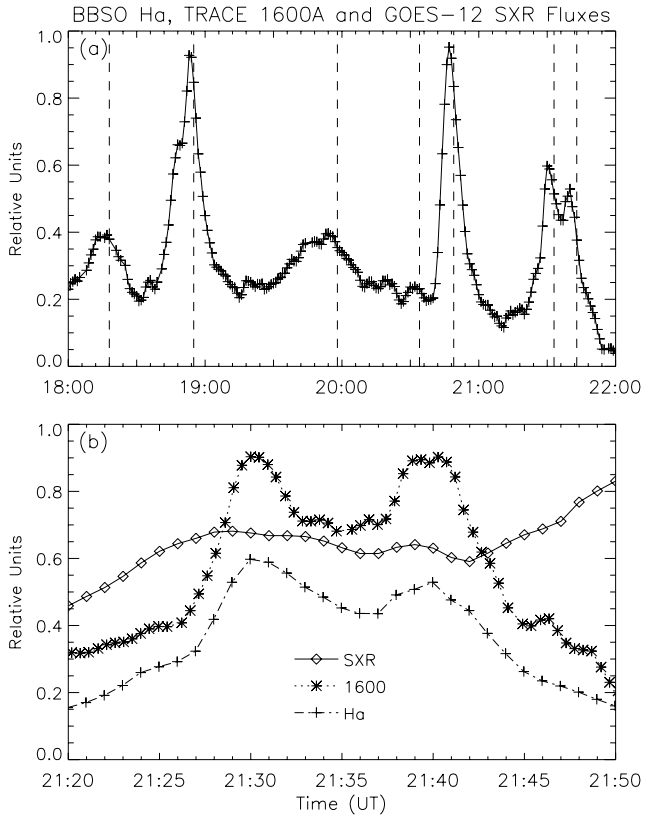

Fig. 6. Panel **a)** time profile of BBSO H_α flux from 18 to 22 UT. Panel **b)** time profiles of GOES soft X-ray (*diamonds; solid line*), TRACE 1600 Å (*asterisks; dotted line*) and BBSO H_α (*pluses; dash-dotted line*) fluxes from 21:20 to 21:50 UT. The dashed lines in panel **a)** indicate the times when the surges first appeared in H_α.

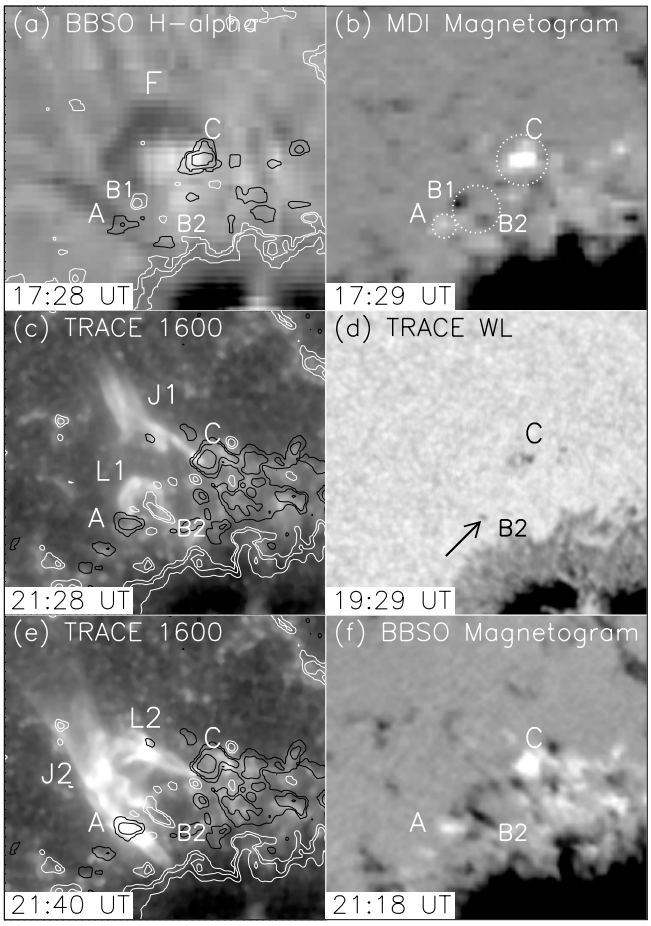

Fig. 7. a) BBSO H_α image overlaid with the contours of the MDI magnetogram **b)**; **b)** MDI magnetogram; **c)**, **e)** TRACE 1600 Å images overlaid with the contours of BBSO magnetogram **f)**; **d)** TRACE white-light image; **f)** BBSO magnetogram. In the panels **a)**, **c)** and **e)**, the white contours are negative (south) polarity, and the black contours are positive (north) polarity. The levels of the contours are ±80, 150, 300 G. The FOV is 95″ × 90″.

patches in H_α images (indicated by the black arrows). Shibata et al. (1992) and Jiang et al. (2007) have reported similar situations in X-ray and EUV jets.

Similar to computing the H_α flux mentioned above, we also calculated the 1600 Å flux in the same region, which is enclosed by the dashed box in the 21:27:37 UT panel of Fig. 4. Panel b in Fig. 6 displays the variation of GOES-12 soft X-ray (SXR) (diamonds; solid line), TRACE 1600 Å (asterisks; dotted line) and BBSO H_α (pluses; dash-dotted line) fluxes from 21:20 to 21:50 UT. Two apparent increases of 1600 Å and H_α fluxes peaked around 21:30 and 21:40 UT reveal that energy is released twice during this period, which should be responsible for events 6 and 7, respectively. As to the SXR flux, there were also two slight enhancements correspondingly. Note the increase of SXR flux after 21:42 UT resulted from a flare of X-ray class M1.0 peaked at 22:08 UT.

For better understanding of the physical essences of events 6 and 7, it would be important to investigate the spatial relationships between the longitudinal magnetic fields and some observational characteristics, including the filament F, the 1600 Å jets (J1, L1, J2 and L2) and the quickly evolving spot. The results are shown in Fig. 7, whose FOV is indicated with the dashed box in the first panel of Fig. 2. In panel a, the BBSO H_α image taken at 17:28 UT was superposed with the contours of an MDI magnetogram observed simultaneously (panel b). We can see that the small arch filament F connected the negative flux B1 and the positive flux C. Comparing the TRACE WL image (panel d) with the longitudinal magnetograms (panels b and f), the position of the small spot emerging around 19:29 UT is found to coincide with that of the growing negative flux B2, which has been described above. In panels c and e, we overlaid the TRACE 1600 Å images with the contours of corresponding BBSO magnetogram (panel f). Some interesting phenomena between the UV jets and the associated flux elements were found. As for event 6, it seems that J1 took root at the flux C and L1 connected with the opposite flux elements A and B2. On the contrary, in event 7, J2 seemed to be rooted in flux A and the two ends of L2 appeared to be located at the opposite flux elements B2 and C, respectively. The distinct different spatial relations of the two 1600 Å jets with the photospheric fields seems to indicate that events 6 and 7 originated from different interaction processes of flux structures. In the next section, we will discuss this at length.

4. Conclusions and discussions

By means of space- and ground-based data, we studied a series of surge activities (events 1–7). Our main observational results are as follows:

1. At H_α, they appeared almost linear ejective structures and reached a maximum projected height of from 38 000 to 220 000 km. They had a transverse velocity of

30–200 km s^{-1} and lasted from a few to tens of minutes. All surges were accompanied by subflares or microflares. In addition, prior to these surges, a small arch filament connecting the opposite magnetic flux elements appeared at the base region. Obviously, it supplied cool material for at least three subsequent surges.

2. In 1600 Å, events 6 and 7 both exhibited the composite structures of bright jets (J1 and J2) and small flaring loops (L1 and L2), whose footpoints seemed to be rooted in the flux elements of alternate positive and negative polarities. A gap with a projected width of $\sim 10^4$ km existed between the UV jets and the loops. In event 6, it can be clearly seen that J1 and L1 continuously widened or thickened at a speed of tens of km s^{-1} when J1 moved along the open field lines. The associated H_α surges 6 and 7 first appeared several minutes later than the 1600 Å jets J1 and J2, respectively.
3. In photosphere, at the base of the surges, it was found that the longitudinal flux elements of opposite magnetic polarities emerged, converged and were canceled by each other. Correspondingly, a small satellite spot emerged, decayed and disappeared during a period of about 2 h in the white-light observations.

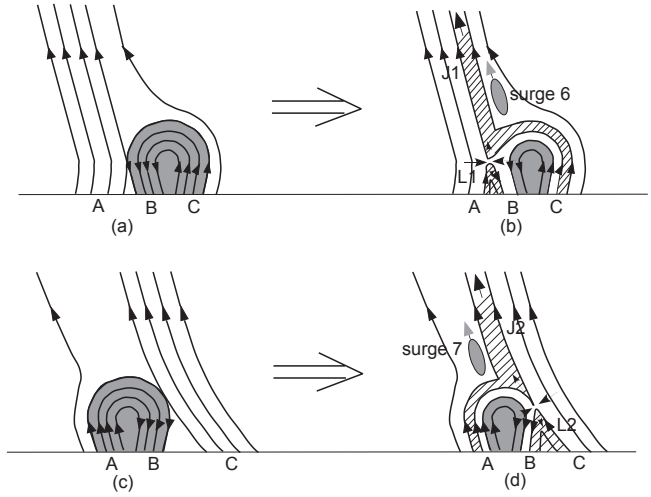

Fig. 8. Two-dimensional cartoons of two magnetic reconnections. The top panels **a)** and **b)** and bottom panels **c)** and **d)** show the approximate occurrence processes of events 6 and 7, respectively.

In this study, although surges 1–7 had very different velocities, lengths and lifetimes, they were very similar in morphology and correlated well with the emergence and cancellation of photospheric flux. This seems to suggest that they had the same physical origin–magnetic reconnection (Shibata et al. 1994; Schmieder et al. 1995; Canfield et al. 1996). In surge events 1, 3 and 4, we can see that partial cool material of the arch filament F ascended and formed the dark surges. Similarly, Wang et al. (2001) presented one case where a filament eruption caused an H_α surge which swept the closed magnetic loop between two active regions. Different from their observations, instead of erupting completely, the filament F in our study disappeared gradually during the series of surges. Its role in the surge activities is very like a bipolar flux, which contained the cool plasma and reconnected with the ambient open field lines (or one leg of a very big closed magnetic loop). This is consistent with the magnetic reconnection surge model. As for events 6 and 7, although before they started, the filament F was basically invisible, some small-scale filamentary structures smaller than the resolution size of $\sim 0\farcs6$ may exist at the base region, only they cannot be detected due to the limited resolution of the H_α data.

In addition, the small flaring loop structures appeared and somewhat separated from the exact footpoints of UV jets in events 2, 6 and 7. These observed features provide direct evidence that they originated from magnetic reconnection. Taking account of the different spatial corresponding relationships with the photospheric longitudinal fields in events 6 and 7, they are very likely to result from different reconnection processes. In Fig. 8, the top panels (a-b) and bottom panels (c-d) show the cartoons of two reconnection processes occurring between the bipolar flux and the ambient unipolar field, which can interpret very well events 6 and 7, respectively. With regard to event 6, due to the converging motion, at first, the reconnection occurred between the negative flux B and the positive flux A. As a consequence, part of the cool plasma was heated by the reconnection and transferred along the open field lines and the reconnected loop, that formed the UV jet J1 and the flaring loop L1, respectively. The widening or thickening variations of J1 and L1 can be explained by the continuous occurrence of the reconnection between the flux elements A and B. On the other hand, another part of the cool plasma was ejected by the sling-shot effect due to reconnection and produced the H_α surge 6. Similarly, in event 7, the reconnection occurred between the negative flux B and the positive flux C and led to the jet J2, the small loop L2 and the H_α surge 7 finally. The main difference between the two events is that the flux structures participating in the reconnections are different: the bipolar flux connected the flux elements B and C and reconnected with the flux A in event 6; while they were located between the flux elements A and B and interacted with the flux C for event 7.

However, in events 6 and 7, the question about the delay of several minutes in the first appearance of H_α surge and UV jet cannot be interpreted well by the reconnection model. Similar phenomena have been reported by other authors (see Schmieder et al. 1994; Alexander & Fletcher 1999; Jiang et al. 2007). In their reports, one possibility was proposed that the later, cooler mass ejections are caused by the cooling of the earlier, hotter jet plasma. In a special case in Jiang et al. (2007), they found that, in a bright EUV jet, dark structures appeared at the location of a future surge. Thus, they thought that the cool material had existed, but its optical thickness is insufficient to be visible in H_α. Besides the two possibilities, another one may be related to the Doppler effect. Since substantial parts of the surge material with high velocities will be shifted out from the H_α line center, we cannot observe all surge material in the H_α line center. The situation often occurs at the onset of surge activity. Chen et al. (2007) just showed one example in which a surge appeared in H_α blue wing almost simultaneously with, while in H_α line center a few minutes later than, its associated EUV plasma ejection. In the future, we expect higher resolution observations in multiwavelength, including in H_α wings, to be acquired for the further test of the magnetic reconnection model of cold and hot plasma ejections.

Acknowledgements. We greatly appreciate the referee for many constructive suggestions. We are grateful to Kejun Li, Pengfei Chen, Zongjun Ning and Zhixing Mei for stimulating discussions. We would like to thank the observing staff at BBSO for making good observations and the TRACE team for providing very nice UV and WL data. Especially, we thank V. B. Yurchyshyn for a lot of kind help on the use of BBSO data. MDI data are courtesy of the SOHO/MDI consortium. SOHO is a project of international cooperation between ESA and NASA. The work is supported by the Natural Science Foundation of China (NSFC under grant 10573033 and 40636031) and by the 973 program (2006CB806303).

References

Alexander, D., & Fletcher, L. 1999, Sol. Phys., 190, 167
Asai, A., Ishii, T. T., & Kurokawa, H. 2001, ApJ, 555, L65
Bruzek, A., & Durrant, C. J. 1977, Illustrated Glossary for Solar and Solar-Terrestrial Physics, Astrophysics ans Space Science Library (Dordrecht: Reidel), 69
Canfield, R. C., Peardon, K. P., Leka, K. D., et al. 1996, ApJ, 464, 1016
Chae, J., Qiu, J., Wang, H., & Goode, P. R. 1999, ApJ, 513, L75
Chen, H. D., Jiang, Y. C., & Ma, S. L. 2007, Sol. Phys., submitted
Chen, H. D., Zhao, S. Q., Li, Q. Y., et al. 2005, ACTA Astron. Sinica, 46, 3, 273
Denker, C., Johannesson, A., Marquette, W., et al. 1999, Sol. Phys., 184, 87
Freeland, S. L., & Handy, B. N. 1998, Sol. Phys., 182, 497
Gu, X. M., Lin, J., Li, K. J., et al. 1994, A&A, 282, 240
Handy, B. N., et al. 1999, Sol. Phys., 187, 229
Jiang, Y. C., Chen, H. D., Li, K. J., et al. 2007, A&A, 469, 331
Kurokawa, H., & Kawai, G. 1993, in The Magnetic and Velocity Fields of Solar Active Region, ed. H. Zirin, G. Ai, & H. Wang (San Francisco: ASP), ASP Conf. Ser., 46, 507
Li, K. J., Li, J., Gu, X. M., & Zhong, S. H. 1996, Sol. Phys., 168, 91
Liu, Y., & Kurokawa, H. 2004, ApJ, 610, 1136
Newton, H. W. 1934, MNRAS, 94, 472
Newton, H. W. 1942, MNRAS, 102, 2
Roy, J. R. 1973, Sol. Phys., 28, 95
Rust, D. M. 1968, in Structure and Development of Solar Active Regions, ed. K. O. Kiepenheuer (Dordrecht: Reidel), IAU Symp., 35, 77
Rust, D. M., Webb, D. E., & McCombie, W. 1977, Sol. Phys., 54, 53
Saba, J. L. R., Gaeng, T., & Tarbell, T. D. 2006, ApJ, 641, 1197
Scherrer, P. H., et al. 1995, Sol. Phys., 162, 129
Schmahl, E. J. 1981, Sol. Phys., 69, 135
Schmieder, B., Mein, P., Martres, M. J., & Tandberg-Hanssen, E. 1984, Sol. Phys., 94, 133
Schmieder, B., Simnett, G. M., Tandberg-Hanssen, E., & Mein, P. 1988, A&A, 201, 327
Schmieder, B., van Driel-Gesztelyi, L., Gerlei, O., & Simnett, G. 1993, Sol. Phys., 146, 163
Schmieder, B., Golub, L., & Antiochos, S. K. 1994, ApJ, 425, 326
Schmieder, B., Shibata, K., Van Driel-Gesztelyi, L., & Freeland, S. 1995, Sol. Phys., 156, 245
Schrijver, C. J., et al. 1999, Sol. Phys., 187, 26
Shibata, K., Ishido, Y., Acton, L. W., et al. 1992, PASJ, 44, L173
Shibata, K., Nitta, N., Strong, K. T., et al. 1994, ApJ, 431, L51
Shimojo, M., Hashimoto, S., Shibata, K., et al. 1996, PASJ, 48, 123
Shimojo, M., Shibata, K., & Harvey, K. L. 1998, Sol. Phys., 178, 379
Spirock, T., Denker, C., Chen, H., et al. 2001, ASP Conf. Ser., 236, 65
Švestka, Z., Fárník, F., Tang, F. 1990, Sol. Phys., 127, 149
Wang, H., Chae, J., Yurchyshyn, V., et al. 2001, ApJ, 559, 1171
Yokoyama, T., & Shibata, K. 1995, Nature, 375, 42
Yokoyama, T., & Shibata, K. 1996, PASJ, 48, 353
Yoshimura, K., Kurokawa, H., & Shine, R. 2003, PASJ, 55, 313
Zhang, J., Wang, J., & Liu, Y. 2000, A&A, 361, 759